Novel in vivo TDP-43 stress reporter models to accelerate drug development in ALS

Ferro, Febe; Wolf, C. Roland; Henstridge, Christopher; Inesta-Vaquera, Francisco

Published in:
Open Biology

DOI:
10.1098/rsob.240073

Publication date:
2024

OPEN BIOLOGY

royalsocietypublishing.org/journal/rsob

Methods and techniques

Cite this article: Ferro F, Wolf CR, Henstridge C, Inesta-Vaquera F. 2024 Novel *in vivo* TDP-43 stress reporter models to accelerate drug development in ALS. *Open Biol.* **14**: 240073.
https://doi.org/10.1098/rsob.240073

Received: 21 March 2024
Accepted: 23 September 2024

Subject Areas:
neuroscience, molecular biology, biotechnology, biochemistry, cellular biology

Keywords:
in vivo, TDP-43, reporters, preclinical models

Author for correspondence:
Francisco Inesta-Vaquera
e-mail: finestavaquera@unex.es

Novel *in vivo* TDP-43 stress reporter models to accelerate drug development in ALS

Febe Ferro[1], C. Roland Wolf[1], Christopher Henstridge[1] and Francisco Inesta-Vaquera[1,2]

[1]Systems and Cellular Medicine, University of Dundee, Dundee DD1 9SY, UK
[2]Department of Biochemistry and Molecular Biology and Genetics, University of Extremadura, Badajoz 06006, Spain

FF, 0009-0007-1960-0208; CRW, 0000-0002-6969-0113; CH, 0000-0002-0393-180X; FI-V, 0000-0002-4579-7418

The development of therapies to combat neurodegenerative diseases is widely recognized as a research priority. Despite recent advances in understanding their molecular basis, there is a lack of suitable early biomarkers to test selected compounds and accelerate their translation to clinical trials. We have investigated the utility of *in vivo* reporters of cytoprotective pathways (e.g. NRF2, p53) as surrogate early biomarkers of the ALS degenerative disease progression. We hypothesized that cellular stress observed in a model of ALS may precede overt cellular damage and could activate our cytoprotective pathway reporters. To test this hypothesis, we generated novel ALS-reporter mice by crossing the hTDP-43tg model into our oxidative stress/inflammation (Hmox1; NRF2 pathway) and DNA damage (p21; p53 pathway) stress reporter models. Histological analysis of reporter expression in a homozygous hTDP-43tg background demonstrated a time-dependent and tissue-specific activation of the reporters in tissues directly associated with ALS, before moderate clinical signs are observed. Further work is warranted to determine the specific mechanisms by which TDP-43 accumulation leads to reporter activation and whether therapeutic intervention modulates reporters' expression. We anticipate the reporter strategy could be of great value in developing treatments for a range of degenerative disorders.

1. Introduction

Age-related diseases account for a high proportion of the total global burden of disease. Degenerative diseases of old age, including cardiovascular disease, stroke, type II diabetes and chronic respiratory conditions, have emerged as the major causes of death worldwide. Of special concern are neurodegenerative conditions including Alzheimer's disease (AD), Parkinson's disease and other dementias, which have been described as the greatest unmet need facing modern medicine [1,2]. Developing new therapies to slow, halt or reverse these pathologies is regarded as a key element in addressing this global health priority. Unfortunately, no prognostic biomarkers of degeneration are available to predict whether a candidate disease-modifying therapy is likely to improve clinical outcome [3]. As a consequence, there is an urgent need for prognostic biomarkers of degeneration that can improve the ability of preclinical research to correctly predict future clinical benefit [4].

One major impediment in developing new treatments of these diseases is the lack of robust models with which to identify and prioritize therapeutic approaches to be tested and then progressed to clinical trials in a timely

THE ROYAL SOCIETY PUBLISHING

manner. The development of early biomarkers prior to the onset of clinical symptoms would at least in part address this issue [5].

ALS is a progressive neurodegenerative disease, characterized by motor neuron loss, which results in paralysis and death 3–5 years after disease onset [6]. At the molecular level, most sporadic and familial ALS cases are characterized neuropathologically by cellular aggregates of transactive response DNA-binding protein 43 kDa (TDP-43) [7]. Furthermore, TDP-43 aggregates are observed in approximately 50% of frontotemporal dementia (FTD), 30% of AD and 20% of Parkinson's disease cases, so understanding its toxic mechanism(s) is essential. The mechanism of TDP-43-induced cell death is associated with the induction of cellular stress; however, the actual stress responses involved (e.g. inflammation, oxidative stress, DNA damage) remain unclear [8]. There is therefore a need to characterize these pathways to aid the development of new treatments for this intractable disease [9].

The mechanisms of TDP-43 aggregation and its associated toxicity (inflammation, oxidative stress and DNA damage) in ALS/FTD are still poorly understood [7,9,10]. To improve our understanding of TDP-43 toxicity, researchers have generated several TPD-43 murine models that mimic human ALS/FTD pathologies. One of these models, the hTDP-43tg, overexpresses human wild-type TDP-43 under the control of the neuronal murine Thy-1 promoter that drives transgene expression in virtually all neurons of the central nervous system from one week after birth [11,12]. Homozygous hTDP-43tg mice express a four- to fivefold induction of hTDP-43 compared with murine TDP-43. Whereas mice hemizygous for the TDP-43 transgene (TDP-43^{het}) are viable, fertile and grossly normal, mice that have two copies of this transgene (TDP-43^{hom}) display profound motor dysfunction, resulting in an inability to walk around P21 and death around P24. This model provides an opportunity to study TDP-43-driven pathology and cell stress in a short time frame.

We have developed a portfolio of reporter mouse models in which the activation of cellular cytoprotective pathways, including inflammation/oxidative stress (NRF2-Hmox1 reporter) and senescence/DNA damage (p53–p21 reporter), can be monitored at single-cell resolution across all organs, tissues and cell types [13–15]. Moreover, the measurements can also be performed non-invasively and in real time. In each model, a short viral DNA sequence, known as a 2A sequence, is exploited to provide multiple reporters expressed (separately) from a single gene promoter. For example, when Hmox1 reporter mice were exposed to inducers of oxidative stress (e.g. paracetamol) or inflammatory mediators (e.g. LPS), a tissue- and cell-specific induction of β-galactosidase reporter activity was observed. Similarly, when the p21 reporter mice were exposed to DNA damage-inducing agents (e.g. gamma-irradiation or cisplatin) an increase of p21 expression was detected at a high level of fidelity and resolution in target tissues. We therefore wanted to explore whether cellular stress resulting from accumulation of hTDP-43, including DNA damage and inflammation, would activate the expression of these reporters in neurons.

In this short communication, we report the generation of a hTDP-43 reporter system that could be applied to test the efficacy of novel therapeutic interventions for motor neuron disease. These mice will be made available to the research community.

2. Methods

2.1. Animals

hTDP-43 animals were purchased from Jackson Lab (B6;SJL-Tg(Thy1-TARDBP)4Singh/J; strain number 012836) and they were described before [11]. hTDP-43_p21 and hTDP-43_Hmox1 reporter mice were generated by crossing hTDP-43 heterozygous (hTDP43^{het}) mice into heterozygous Hmox1 (HOTT^{het}) or p21 (p21^{het}) reporter mice [13]. Mice were housed in open-top cages in temperature-controlled rooms at 21°C, with 45–65% relative humidity and 12 h/12 h light/dark cycle. Mice had ad libitum access to food (R&M No. 1 for stock females; R&M No. 3 for mating females; Special Diet Services, Essex, UK) and water. Animals were regularly subjected to health and welfare monitoring as standard (twice daily). Environmental enrichment was provided for all animals. All animal work described was approved by the Welfare and Ethical Use of Animals Committee of the University of Dundee. No regulated procedures were conducted in these animals.

The severity of hTDP-43 mice phenotype was assessed according to the established scoring system. Briefly, a score of 0 corresponds to mice that when suspended by the tail, both hindlimbs were consistently splayed outward, away from the abdomen. At this score system, mouse moves normally with body weight supported on all limbs; a score of 1 was achieved when mice suspended by the tail retracted one hindlimb toward the abdomen for more than 50% of the time suspended. Mice at this score had a mild tremor or a limp while walking; a score of 2 was given to those mice that when suspended by the tail, both limbs are partially retracted towards the body for 50% of the time suspended. Mice at this score show severe tremor and/or limp, or the feet point away from the body during locomotion ('duck feet'); finally, a score of 3 is reached when mice are suspended by the tail, both limbs are fully retracted for more than 50% of the time suspended and/or the mouse has difficulty moving forward and drags its abdomen along the ground. Throughout our studies, no animals progressed to score 2.

2.2. Genotyping

Genotyping for the p21 and HOTT strains was performed as described before [16] and according to instructions in the case of hTDP-43 mice. The primers used were as follows: Hmox1 reporter: HO1-KI Fwd, 5′-GCTGTATTACCTTTGGAGCAGG-3′; HO-1-KI Rvr, 5′-CCAAAGAGGTAGCTAATTCTATCAGG-3′; p21 reporter: p21-KI Fwd, 5′-GCTACTTGTGCTGTTTGCACC-3′; p21-KI Rvr, 5′-TCAAGGCTTTAGGTTCAAGTACC-3′; hTDP-43 common primer: 5′-TGAAATCCGGGTGGTATTGG-3′; hTDP-43 (wild-type allele): 5′-GGTGAGTTTAACCTTCAAGGGCT-3′; hTDP-43 (transgene): 5′-AGCTTGCTAGCGGATCCAGAC-3′.

2.3. Tissue harvesting and processing for cryo-sectioning

Mice were perfused with phosphate-buffered saline (PBS) followed by 4% paraformaldehyde in 0.1 M PBS pH 7.2–7.4 (flow rate 5 ml min^{-1}). Brains were harvested, halved and post-fixed in 4% paraformaldehyde (PFA) overnight for IHF and for 3 h for LacZ staining. Brains were sectioned using a vibratome (Leica VT1000S). Superglue (LocTite SuperAttak Gel) was used to attach the brain to the cutting surface vertically, so the cerebral cortex was facing up. Tissues were immersed in a PBS bath. Blades Gillette 'Wilkinson Sword' were used. Sections were cut at 40 µm thickness and saved in a 24-well tissue-culture dish filled with 1× PBS, 0.5% sodium azide (5 sections per well). Sections were picked up with a paintbrush. One section per well was mounted on slides for IHC. Tissues preserved for β-galactosidase staining were rapidly harvested postmortem and processed by immersion fixation in 4% PFA (brain, small intestine) for 2 h, 3% neutral-buffered formalin (liver) for 3 h or Mirsky's fixative (rest of tissues) for 24 h and subsequently cryoprotected for 24 h in 30% (w/v) sucrose in PBS at 4°C. Organs were embedded in Shandon M-1 Embedding Matrix in a dry ice–isopentane bath. Sectioning was performed on an OFT5000 cryostat (Bright Instrument Co.). With the exception of lung (14 µm) and brain (20 µm) sections, all sections were cut at 10 µm thickness.

2.4. *In situ* β-galactosidase staining, histochemistry and quantitation

Sections were rehydrated in PBS at room temperature for 15 min before being incubated overnight at 37°C in X-gal staining solution: PBS (pH 7.4) containing 2 mM $MgCl_2$, 0.01% (w/v) sodium deoxycholate, 0.02% (v/v) Igepal-CA630, 5 mM potassium ferricyanide, 5 mM potassium ferrocyanide and 1 mg ml^{-1} 5-bromo-4-chloro-3-indolyl β-D-galactopyranoside. On the following day, slides were washed in phosphate buffer solution, counterstained in Nuclear FastRed (Vector Laboratories) for 4 min, washed twice in distilled water for 2 min and dehydrated through 70% and 95% ethanol (4.5 and 1 min, respectively) before being incubated in Histoclear (VWR) for 3 min, air-dried and mounted in DPX mountant (Sigma). Because the β-gal protein contains a nuclear localization signal, it is localized specifically in cell nuclei [15]. The software ImageJ v1.53n and plug-in 'Colour deconvolution2' was used for quantitative image analysis of the β-gal activity. The analysis was based on microscope images that were acquired with a Zeiss Axio Observer (Carl Zeiss, Jena, Germany). The software automatically determined the area of blue colouration within the microscopic image. Subsequently, the percentage of the area of LacZ positive staining of each acquired microscope image was determined.

2.5. Tissue immunofluorescence

Tissue slices were washed in 0.1 M phosphate buffer before submerging in 10% sucrose for 15 min followed by 30% sucrose at room temperature for 3 h. Slices were wrapped in tin foil and permeabilization was performed by four freeze/thaw cycles above liquid nitrogen and finally placed in 0.1 M phosphate buffer. After peroxidase blocking with 1% H_2O_2 slices were washed in 0.1 M phosphate buffer and tris buffered saline solution and antigen blocking for 45 min at room temperature with 1% human serum albumin. Primary antibodies were incubated overnight at 4°C before TBS washing and incubation with secondary antibody (1 h room temperature). After phosphate buffer washing, sections were allowed to slightly dry and mounted with Vectashield. Primary antibodies used: TDP-43 (Abcam, ab133547 Rabbit monoclonal (EPR5811)); GFAP (Proteintech, 16825-1-AP Rabbit/IgG); Parvalbumin (Swant, PV27 rabbit).

2.6. Image acquisition and quantitation

Images from immunolabelled tissues were acquired using a Delta Vision Elite high-resolution microscope with a Leica 20× APO 1.4 lens. Convoluted Z-stack images were acquired from multiple fields. Exposure and laser intensity were fixed before proceeding with fluorescence quantification to allow direct comparisons between sections. ImageJ (v2.0.0, NIH) analysis software was used for relative fluorescence intensity quantitation. Image analysis was performed as previously described [17]. Briefly, colour channels were split, and regions of interest (ROI) were selected. Measurement values for area, integrated density, mean/maximum/minimum grey value were recorded. A minimum of 10 background ROIs were selected. Corrected total cell fluorescence (CTFC) was calculated: integrated density – (area of selected cell × mean fluorescence of background readings) [17]. CTCF values were obtained by measuring the fluorescence intensity of TDP-43 in selected cells across three different fields of view in slides from individual experimental animal. The obtained values were then averaged for each ROI, and subsequently plotted as $hTDP\text{-}43^{wt}$_$HOTT^{het}$ versus $hTDP\text{-}43^{hom}$_$HOTT^{het}$ and statistical analysis (one-sided unpaired Student *t*-tests) was performed using GraphPad Prism 10.0.2.

3. Results and discussion

To establish whether the *in vivo* reporters of DNA damage (p21) or oxidative stress/inflammation (Hmox1) act as early biomarkers of TDP-43-induced pathologies, hTDP-43 mice were crossed into $HOTT^{hom}$ as well as $p21^{hom}$ reporter mice resulting in the TDP-43_HOTT or TDP-43_p21 lines. These mice were used to generate $hTDP\text{-}43^{hom}$_HOTT and $hTDP\text{-}43^{hom}$_p21 mice. The average litter sizes resulting from these crosses was approximately 8 ± 2 pups and within normal Mendelian ratios. For ethical reasons, mice were only kept until they were 17 days old. At this stage, $hTDP\text{-}43^{hom}$ mice showed an expected phenotype of mild

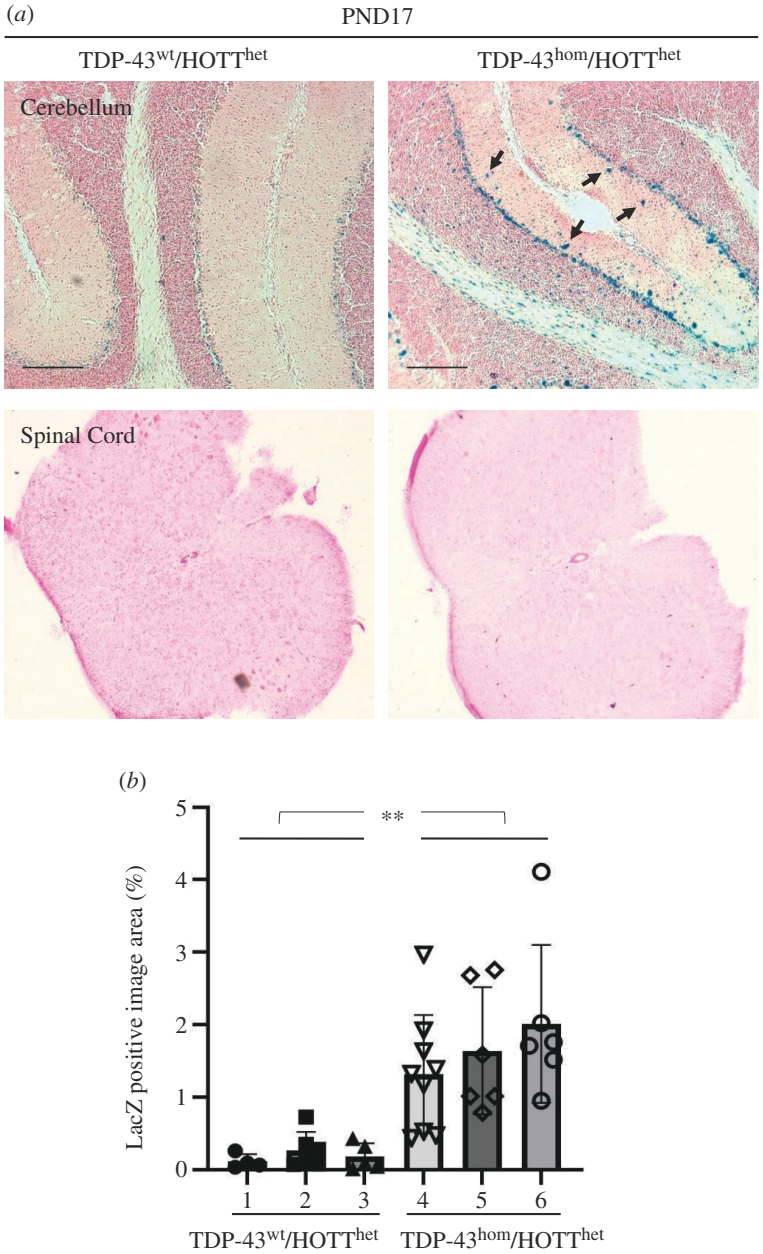

Figure 1. Demonstration of the HOTT reporter model utility to detect cellular stress associated with hTDP-43 accumulation. (*a*) Representative images of LacZ staining in cerebellum (upper row) or lumar spinal cord (lower row) sections from triplicated mice of indicated genotypes. PND17, post-natal day 17. Black scale bar, 40 µm. Black arrows indicate positive cells for LacZ staining. (*b*) Quantitation of LacZ positive area in a minimum of six images from cerebellum sections of indicated genotypes. Numbers indicate individual mice. %, positive area referred to total image area. $^{**}p < 0.005$.

tremor and or a limp while walking (score 1). A complete list of collected tissues from different genotypes and animal age is provided (electronic supplementary material, table S1).

Histological analysis of post-natal day 17 (PND17) TDP-43^{hom}-HOTT^{het} reporter mice demonstrated a profound induction of reporter expression in a disease relevant tissue, the cerebellum (figure 1*a*) [18–20]. The basal reporter expression and the increased signal due to hTDP-43 accumulation was similar in male and female so animals of both sexes were included in the reporter analysis of different age groups. We found a cell specific activation of the reporter in the cerebellum and typically in what appear to be PV+ cells, such as Purkinje (Purkinje layer) and basket (molecular layer) cells. Immunofluorescence staining of hTDP-43^{wt} or hTDP-43^{hom} cerebellum samples with parvalbumin (general GABAergic cell marker, including Purkinje and basket cells) and GFAP (astrocytes) markers confirmed the likely identity of these cells in the reporter-positive region (electronic supplementary material, figure S1A). In addition, quantitative analysis of hTDP-43 immunofluorescence staining demonstrated a twofold increased expression of the transgene in this area, consistent with previous expression analysis reports for this line (electronic supplementary material, figure S1B) [11]. In addition, LacZ-positive area was quantified in cerebellum sections from three independent mice in each genotype (figure 1*b*). We observed a very significant increase in LacZ positive signal in hTDP-43^{hom} mice. However, we caveat that LacZ assays inform on transcriptional changes on a qualitative basis. As a consequence, contrary to fluorescently tagged proteins, LacZ staining quantitation may not correlate with protein expression levels.

We extended our reporter expression analysis to other disease relevant areas of the central nervous system and peripheral organs. These included the spinal cord, cortex and hippocampus (figure 1; electronic supplementary material, figure S2).

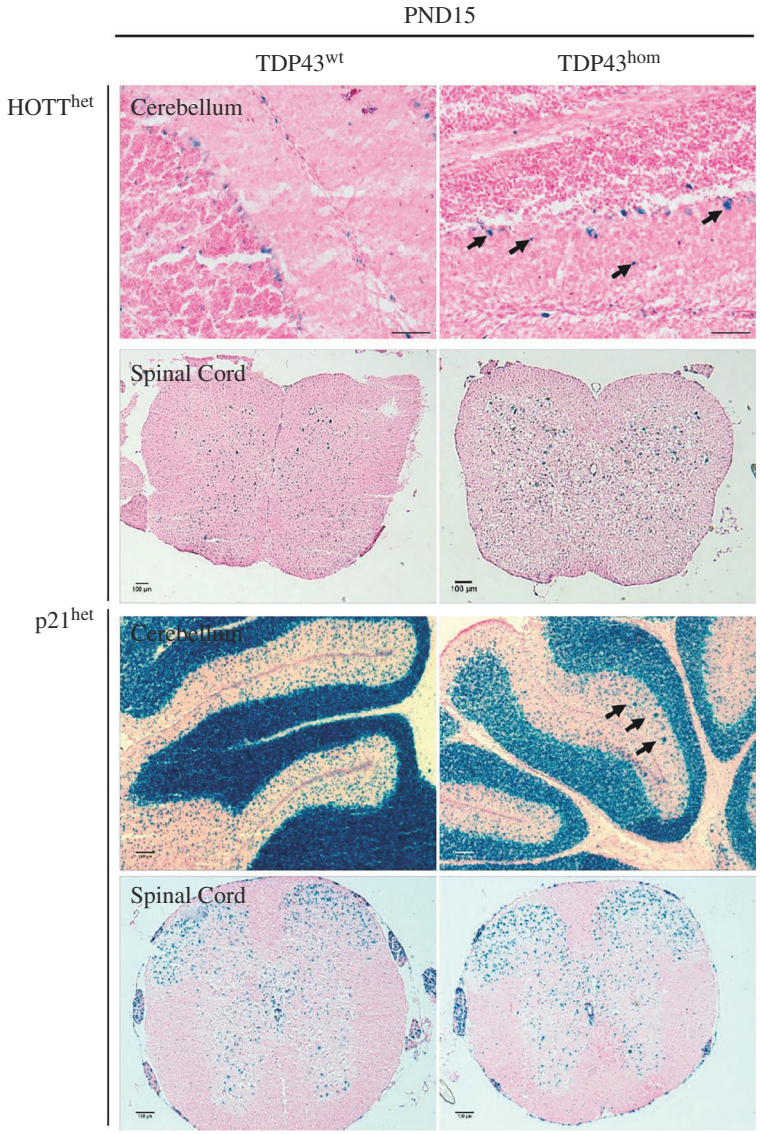

Figure 2. Early detection of hTDP-43 associated stress responses using the HOTT and p21 reporter models. Representative images of LacZ staining in cerebellum and spinal cord sections of Hmox1 (upper rows) or p21 (lower rows) reporters from triplicated mice of indicated genotypes. PND15, post-natal day 15. Black scale bar, 100 µm. Black arrows indicate positive cells for LacZ staining.

Positive β-gal staining was observed in hTDP-43^{wt}-HOTT^{het} mice as previously described in dentate gyrus and cortex regions [13]. Differential expression of the reporter was not observed between the experimental groups in areas of spinal cord (figure 1). However, the interpretation of these data was confounded by the fact that a variable reporter expression in this tissue was observed irrespective of the genotype. The significance of basal Hmox1 expression in these cells warrants further investigation.

The reporter activation in hTDP-43^{hom} mice occurred at a clinical score of 1, i.e. which precedes overt morbid phenotypes. Therefore, reporter activation provides a more refined endpoint to assess the effectiveness of therapeutic interventions aimed at reducing hTDP-43 accumulation [21]. In addition, because changes in reporter expression were consistent between individual mice, the number of mice required to obtain statistical significance relative to current approaches is reduced. We would caveat that the β-gal reporter assay should be interpreted as a qualitative marker for pathway activation, which does not inform on the strength of the response. Indeed, when we co-stained hTDP-43^{hom} _HOTT^{het} cerebellum sections with a β-gal antibody we did not observe a robust signal, suggesting that the expression of the β-gal reporter is below the limits of antibody-based detection. As a staining control, we observed positive β-gal in the nucleus of liver cells in samples previously generated in our laboratory (not shown).

To investigate whether reporter activation occurs at earlier time points, we analysed samples derived from PND15 pups in hTDP-43^{hom}-HOTT^{het} and hTDP-43^{hom}-p21^{het} mice (figure 2; electronic supplementary material, figure S4). A mild but consistent activation of the reporter in the cerebellum of hTDP-43^{hom}-HOTT^{het} mice was detected, similar of that observed at later stages. Unfortunately, the very high basal expression of the p21 reporter in the cerebellum precluded robust results with this mouse line. However, we observed distinctive positive (potentially basket) cells in the cerebellum of p21 reporter mice, similar to those observed in the HOTT line, suggesting this pathway is also activated in hTDP-43^{hom} mice (figure 2). No differential reporter activation was observed in other areas of the brain (electronic supplementary material, figure S4).

Remarkably, we have previously observed an enhanced sensitivity of PV+ cells in a novel TDP-43 mouse with a single point mutation inserted within the mouse TDP-43 gene (TDP-43$^{Q331K/Q331K}$) [22]. In this model, a reduction in the number of parvalbumin interneurons correlated with regional brain atrophy in mutant mice at both 5 and 20 months of age. Interestingly,

this model also presents with early cerebellar atrophy, so together, we present evidence of a potential contribution of cerebellar PV+ cells to the pathogenesis of ALS. Further work is warranted to investigate whether the activation of the Hmox1 (oxidative stress/inflammation) or p21 (DNA damage) pathways are molecularly linked to the loss of PV cells in other TDP-43 mouse models and ALS patients.

We further investigated a potential hTDP-43 transgene dosage effect. We analysed hTDP-43^{het} reporter expression in tissues of mice up to 40 weeks of age. No changes in β-gal staining were observed in any of the tissues studied, including in the cerebellum, spinal cord, cortex and hippocampus (electronic supplementary material, figure S4).

The data from our studies demonstrate the activation of specific TDP-43-dependent cell stress response pathways in a disease relevant cell population [19,20,23,24]. It is important to note that the toxicity of severe phenotypes can lead to simultaneous activation of multiple stress pathways (toxicity burst), making it difficult to define the molecular hierarchy of these events [25]. Our reporter data demonstrate the early induction of oxidative stress, inflammation (pathways leading to Hmox1) and DNA damage (p21 reporter) in TDP-43 pathologies. However, other cellular stress responses have been associated with the accumulation of hTDP-43, including integrated stress response [26], endoplasmic reticulum stress and the unfolded protein response [27]. Therefore, whether the pathways leading to Hmox1 or p21 expression are a cause or a consequence of TDP-43-related changes remains to be studied. Nevertheless, it will be important to identify the exact mechanism(s) linking hTDP-43-dependent and -independent expression with the reporter activation in critical ALS-related brain areas. Indeed, some therapies being developed to treat ALS are targeted at the NRF2 pathway, which is a major regulator of the Hmox1 gene [28].

In summary, the reporters generated offer a novel method to understand the biological basis of disease and to test novel therapeutic approaches in ALS at the physiological level. Because the reporter can be used as a biomarker of TDP-43 accumulation, researchers will be able to easily track changes in disease progression at the single-cell resolution across organs and tissues. These reporters therefore represent the first prognostic biomarkers of degeneration that can improve the ability of preclinical research to correctly predict future clinical benefit. In particular, this work demonstrates the potential use of our stress reporter approaches to accelerate finding new treatments for early stages of degenerative diseases prior to any perceptible deleterious phenotype. We will support the use of hTDP-43-HOTT mice as a new tool for interventional studies in TDP-43-dependent diseases. The accessibility of these models will accelerate testing molecules/approaches and their PK profiles before human trials.

Ethics. All animal work described was approved by the Welfare and Ethical Use of Animals Committee of the University of Dundee.

Data accessibility. This article has no additional data.

Declaration of AI use. We have not used AI-assisted technologies in creating this article.

Authors' contributions. F.F.: data curation, formal analysis, investigation, methodology; C.R.W.: conceptualization, resources, supervision, writing—review and editing; C.H.: conceptualization, formal analysis, funding acquisition, investigation, methodology, resources, supervision, writing—review and editing; F.I.-V.: conceptualization, formal analysis, funding acquisition, investigation, methodology, project administration, supervision, writing—original draft, writing—review and editing.

All authors gave final approval for publication and agreed to be held accountable for the work performed therein.

Conflict of interest declaration. We declare we have no competing interests.

Funding. This research was funded by an Alzheimer's Research UK (ARUK-PPG2020A-003) and MND Scotland (RC21-06) pilot grants awarded to F.I.-V./C.H. F.F. is a recipient of the Daphne Merrills PhD Studentship, jointly funded by Brain Research UK and Neuroscience Foundation.

Acknowledgements. We thank Prof. Tom Gillingwater and Dr Helena Chaytow for discussions, genotyping and animal scoring advice. We also thank Chris Henstridge laboratory members for their advice on tissue processing and analysis.

References

1. Feigin VL *et al*. 2020 The global burden of neurological disorders: translating evidence into policy. *Lancet Neurol*. **19**, 255–265. (doi:10.1016/S1474-4422(19)30411-9)
2. Feigin VL, Vos T. 2019 Global burden of neurological disorders: from global burden of disease estimates to actions. *Neuroepidemiology* **52**, 1–2. (doi:10.1159/000495197)
3. Hansson O. 2021 Biomarkers for neurodegenerative diseases. *Nat. Med*. **27**, 954–963. (doi:10.1038/s41591-021-01382-x)
4. Petrov D, Mansfield C, Moussy A, Hermine O. 2017 ALS clinical trials review: 20 years of failure. Are we any closer to registering a new treatment? *Front. Aging Neurosci*. **9**, 68. (doi:10.3389/fnagi.2017.00068)
5. Tan RH, Ke YD, Ittner LM, Halliday GM. 2017 ALS/FTLD: experimental models and reality. *Acta Neuropathol*. **133**, 177–196. (doi:10.1007/s00401-016-1666-6)
6. Masrori P, Van Damme P. 2020 Amyotrophic lateral sclerosis: a clinical review. *Eur. J. Neurol*. **27**, 1918–1929. (doi:10.1111/ene.14393)
7. Neumann M *et al*. 2006 Ubiquitinated TDP-43 in frontotemporal lobar degeneration and amyotrophic lateral sclerosis. *Science* **314**, 130–133. (doi:10.1126/science.1134108)
8. Mackenzie IRA, Neumann M. 2016 Molecular neuropathology of frontotemporal dementia: insights into disease mechanisms from postmortem studies. *J. Neurochem*. **138 Suppl. 1**, 54–70. (doi:10.1111/jnc.13588)
9. Kawakami I, Arai T, Hasegawa M. 2019 The basis of clinicopathological heterogeneity in TDP-43 proteinopathy. *Acta Neuropathol*. **138**, 751–770. (doi:10.1007/s00401-019-02077-x)
10. Hasegawa M *et al*. 2008 Phosphorylated TDP-43 in frontotemporal lobar degeneration and amyotrophic lateral sclerosis. *Ann. Neurol*. **64**, 60–70. (doi:10.1002/ana.21425)
11. Wils H *et al*. 2010 TDP-43 transgenic mice develop spastic paralysis and neuronal inclusions characteristic of ALS and frontotemporal lobar degeneration. *Proc. Natl Acad. Sci. USA* **107**, 3858–3863. (doi:10.1073/pnas.0912417107)
12. Becker LA *et al*. 2017 Therapeutic reduction of ataxin-2 extends lifespan and reduces pathology in TDP-43 mice. *Nature* **544**, 367–371. (doi:10.1038/nature22038)
13. Iñesta Vaquera F, Ferro F, McMahon M, Henderson CJ, Wolf CR. 2022 Potential of *in vivo* stress reporter models to reduce animal use and provide mechanistic insights in toxicity studies. *F1000Research* **11**, 1164. (doi:10.12688/f1000research.123077.1)
14. McMahon M, Frangova TG, Henderson CJ, Wolf CR. 2016 Olaparib, monotherapy or with ionizing radiation, exacerbates dna damage in normal tissues: insights from a new p21 reporter mouse. *Mol. Cancer Res*. **14**, 1195–1203. (doi:10.1158/1541-7786.MCR-16-0108)

15. McMahon M, Ding S, Acosta-Jimenez LP, Frangova TG, Henderson CJ, Wolf CR. 2018 Measuring *in vivo* responses to endogenous and exogenous oxidative stress using a novel haem oxygenase 1 reporter mouse. *J. Physiol.* **596**, 105–127. (doi:10.1113/JP274915)
16. Inesta-Vaquera F, Navasumrit P, Henderson CJ, Frangova TG, Honda T, Dinkova-Kostova AT, Ruchirawat M, Wolf CR. 2021 Application of the *in vivo* oxidative stress reporter Hmox1 as mechanistic biomarker of arsenic toxicity. *Environ. Pollut.* **270**, 116053. (doi:10.1016/j.envpol.2020.116053)
17. McCloy RA, Rogers S, Caldon CE, Lorca T, Castro A, Burgess A. 2014 Partial inhibition of Cdk1 in G 2 phase overrides the SAC and decouples mitotic events. *Cell Cycle* **13**, 1400–1412. (doi:10.4161/cc.28401)
18. Pickles S *et al*. 2022 Evidence of cerebellar TDP-43 loss of function in FTLD-TDP. *Acta Neuropathol. Commun*. **10**, 107. (doi:10.1186/s40478-022-01408-6)
19. Chipika RH, Mulkerrin G, Pradat PF, Murad A, Ango F, Raoul C, Bede P. 2022 Cerebellar pathology in motor neuron disease: neuroplasticity and neurodegeneration. *Neural Regen. Res*. **17**, 2335–2341. (doi:10.4103/1673-5374.336139)
20. Kabiljo R, Iacoangeli A, Al-Chalabi A, Rosenzweig I. 2022 Amyotrophic lateral sclerosis and cerebellum. *Sci. Rep*. **12**, 12586. (doi:10.1038/s41598-022-16772-5)
21. Chaytow H *et al*. 2022 Targeting phosphoglycerate kinase 1 with terazosin improves motor neuron phenotypes in multiple models of amyotrophic lateral sclerosis. *EBioMedicine* **83**, 104202. (doi:10.1016/j.ebiom.2022.104202)
22. Lin Z *et al*. 2021 MRI-guided histology of TDP-43 knock-in mice implicates parvalbumin interneuron loss, impaired neurogenesis and aberrant neurodevelopment in amyotrophic lateral sclerosis-frontotemporal dementia. *Brain Commun*. **3**, fcab114. (doi:10.1093/braincomms/fcab114)
23. Baradaran-Heravi Y, Van Broeckhoven C, van der Zee J. 2020 Stress granule mediated protein aggregation and underlying gene defects in the FTD-ALS spectrum. *Neurobiol. Dis*. **134**, 104639. (doi:10.1016/j.nbd.2019.104639)
24. McCauley ME, Baloh RH. 2019 Inflammation in ALS/FTD pathogenesis. *Acta Neuropathol*. **137**, 715–730. (doi:10.1007/s00401-018-1933-9)
25. Escher BI, Henneberger L, König M, Schlichting R, Fischer FC. 2020 Cytotoxicity burst? Differentiating specific from nonspecific effects in Tox21 *in vitro* reporter gene assays. *Environ. Health Perspect.* **128**, 77007. (doi:10.1289/EHP6664)
26. Luan W *et al*. 2023 Early activation of cellular stress and death pathways caused by cytoplasmic TDP-43 in the rNLS8 mouse model of ALS and FTD. *Mol. Psychiatry* **28**, 2445–2461. (doi:10.1038/s41380-023-02036-9)
27. de Mena L, Lopez-Scarim J, Rincon-Limas DE. 2021 TDP-43 and ER stress in neurodegeneration: friends or foes? *Front. Mol. Neurosci*. **14**, 772226. (doi:10.3389/fnmol.2021.772226)
28. Tarot P, Lasbleiz C, Liévens JC. 2024 NRF2 signaling cascade in amyotrophic lateral sclerosis: bridging the gap between promise and reality. *Neural Regen. Res*. **19**, 1006–1012. (doi:10.4103/1673-5374.385283)